https://doi.org/10.5194/egusphere-2025-2574
Preprint. Discussion started: 13 June 2025

The ENSO-driven bias in the assessment of long-term cloud feedback to global warming

Huan Liu[1], Ilan Koren[2], Orit Altaratz[2], Shutian Mu[1]

[1]College of Meteorology and Oceanography, National University of Defense Technology, Changsha, 410073, China
[2]Department of Earth and Planetary Sciences, Weizmann Institute of Science, Rehovot, 76100, Israel

Correspondence to: Huan Liu (huanliu@nudt.edu.cn)

Abstract. Accurately assessing the cloud feedback to global warming is essential for producing reliable climate projections. Linear regression analysis is a widely used method for this purpose, offering a straightforward approach for examining the relationship between cloud radiative effects and global mean surface temperature. However, the El Niño–Southern Oscillation (ENSO) can introduce a significant bias in these estimations, which is often overlooked due to ENSO's relatively short periodicity. Using 72 years of reanalysis data and 150 years of simulations by 12 global climate models, this study demonstrates that ENSO can produce a bias of comparable magnitude to the estimated cloud feedback, over decades and even centuries. By providing a detailed spatial and temporal analysis of this bias, our findings underscore the importance of accounting for and removing the ENSO's influence to improve the accuracy of cloud feedback assessment in the context of global warming.

1 Introduction

Clouds, which cover over 50% of the Earth's surface, play a critical role in regulating the Earth's energy budget (Stubenrauch et al., 2013). They reflect incoming solar radiation (Short Wave Cloud Radiative Effect, CRE_{SW}) and trap outgoing terrestrial radiation (Long Wave Cloud Radiative Effect, CRE_{LW}), resulting in a net cooling effect of approximately 20 W m^{-2} at the top of the atmosphere (net Cloud Radiative Effect, CRE_{net}) (Stephens et al., 2012). This fundamental role makes cloud response to global warming (cloud feedback) a key factor in climate predictions (Zelinka et al., 2020). However, both the magnitude and sign (positive for additional warming, negative for cooling) of cloud feedback remain uncertain, contributing to significant discrepancies in estimates of equilibrium climate sensitivity (Forster et al., 2021).

One major source of the uncertainty in estimates of cloud feedback to global warming is the natural climate variability , caused by phenomena like the Atlantic Multi-decadal Variability, the Pacific Decadal Oscillation, and the El Niño-Southern Oscillation (ENSO) (Li et al., 2021), all of which can introduce different spatial and temporal bias across different regions and periods (Forster et al., 2021). The ENSO is characterized by anomalous sea surface temperature and sea-level pressure in the tropical Pacific, acting on relatively short timescales and dominating seasonal to interannual timescales (Neelin et al., 1998). By modulating the atmospheric dynamics and thermodynamics (Davey et al., 2014; Taschetto et al., 2020), ENSO can affect cloud properties (Park and Leovy, 2004; Eleftheratos et al., 2011; Teng et al., 2014; Madenach et al., 2019; Liu et al., 2023)

https://doi.org/10.5194/egusphere-2025-2574
Preprint. Discussion started: 13 June 2025

and cloud radiative effects (Chen et al., 2000; Yang et al., 2016). Previous studies have identified an ENSO signature, on a global scale, in both the long-term warming trend (e.g., Penland and Matrosova, 2006; Compo and Sardeshmukh, 2010) and cloud feedback estimates (referred to as ENSO-related bias, hereafter) (e.g., Zhou et al., 2015; Richardson et al., 2022; Uribe et al., 2022; Jin et al., 2024). For example, Richardson et al. (2022) proposed that the ENSO-related bias may affect estimated linear trends over short time windows of up to about 10 years. Jin et al. (2024) found that the seasonally asymmetric patterns of cloud feedback are controlled primarily by ENSO. Nevertheless, the full influence of ENSO on cloud feedback in the context of global warming is still unknown and often overlooked due to the ENSO's relatively short periodicity (i.e., 2–7 years) (Hope et al., 2017), which masks its long-term effect on cloud feedback estimates.

For addressing this knowledge gap, we apply a regression-based de-ENSO method to quantify the spatial distribution and timescales of the ENSO-related bias in cloud feedback estimates under global warming. The paper is organized as follows: Section 2 describes the datasets and methodologies used in the analysis, Section 3 discusses the key findings, and Section 4 summarizes the main conclusions.

2 Materials and methods

2.1 Datasets

This study uses 72 years of reanalysis data from the ERA5 dataset and long-term (150 years) simulations by 12 Global Climate Models (GCM). Based on which, the Oceanic Niño Index (ONI) is derived for measuring ENSO activity as it is NOAA's primary indicator for monitoring ENSO's oceanic signal and is widely used in ENSO-related studies (Glantz and Ramirez, 2020). A period of large positive or negative ONI values indicates an intense warm or cold phase of ENSO (i.e., the El Niño or La Niña event, characterized by an unusual warming or cooling of the central and eastern tropical Pacific Ocean surface waters) (Neelin et al., 1998).

The datasets we use: (1) ERA5 data (January 1950–December 2021). The primary analysis uses monthly ERA5 data (Hershach et al., 2023), a well validated and widely used dataset for studying climate trends, produced by the European Centre for Medium-Range Weather Forecasts (ECMWF) (Hersbach et al., 2020; Gulev et al., 2021). ERA5 data has shown strong agreement with observed cloud properties across both weather and climate scales (Liu et al., 2023; Yao et al., 2020; Binder et al., 2020). The analyzed variables include sea surface temperature, air temperature at 2 meters, Top net Solar Radiation (TSR; the incoming minus the outgoing solar radiation at the top of the atmosphere), Top net Solar Radiation-Clear sky (TSRC; similar to RST but assuming clear sky conditions), Top net Thermal Radiation (TTR; similar to TSR but for thermal radiation), and Top net Thermal Radiation-Clear sky (TTRC; similar to TSRC but for thermal radiation). The original ERA5 resolution (0.25°) was averaged to 2° to reduce computational demands.

(2) GCM simulations (the historical and the abrupt-4×CO_2 experiments). Long-term simulations by 12 GCMs that participated in the Cloud Feedback Model Intercomparison Project of the sixth phase of the Coupled Model Intercomparison Project (CFMIP-3/CMIP6) (Webb et al., 2017). All the selected GCM simulations usethe variant label “r1i1p1f1”, which refers to a

https://doi.org/10.5194/egusphere-2025-2574
Preprint. Discussion started: 13 June 2025

specific experiment configuration within the CMIP6 model run: the first realization with the first set of initial conditions, physics parameterizations, and external forcing conditions. As shown in Table 1, the analyzed simulations include the outputs of the historical and the abrupt-4×CO_2 experiments (Eyring et al., 2016). The historical experiment spans from 1850 to 2014 and is designed to provide insights into how the observed natural and anthropogenic factors have shaped current climate conditions. In this study, the period of 01.1950–12.2014 is analyzed for generalizing the results obtained by the ERA5 data. The abrupt-4×CO_2 experiment is a baseline experiment of the Diagnostic, Evaluation and Characterization of Klima (DECK) experiments that offers a minimum simulation period of 150 years. It is designed to evaluate the immediate climate response to a sudden quadrupling of the prescribed pre-industrial atmospheric CO_2 concentration and hence is widely used for assessing cloud feedback in the context of global warming. The first 150 years in the simulations are used to investigate the ENSO-related bias in cloud feedback estimates. Similar to ERA5 data, the analyzed variables include tas (air temperature at 2 meters), rsut (like TSR), rsutcs (like TSRC), rlut (like TTR), and rlutcs (like TTRC). All GCM simulations are also resampled to a spatial resolution of 2°.

Table 1: Information of the 12 GCM simulations.

GCM	Center	Country	Data Version		Data DOI
			Historical	Abrupt-4×CO_2	
E3SM-1-0	UCSB, E3SM-Project, UCI	USA	v20190913	v20190718	10.22033/ESGF/CMIP6.2294
CESM2	NCAR	USA	v20190308	v20190927	10.22033/ESGF/CMIP6.2185
BCC-CSM2-MR	BCC	China	v20181126	v20181016	10.22033/ESGF/CMIP6.1725
CanESM5	CCCma	Canada	v20190429	v20190429	10.22033/ESGF/CMIP6.1303
MRI-ESM2-0	MRI	Japan	v20190222	v20190308	10.22033/ESGF/CMIP6.621
IPSL-CM6A-LR	IPSL	France	v20180803	v20190118	10.22033/ESGF/CMIP6.1534
TaiESM1	AS-RCEC	China	v20200623	v20200310	10.22033/ESGF/CMIP6.9684
GFDL-CM4	NOAA-GFDL	USA	v20180701	v20180701	10.22033/ESGF/CMIP6.1402
GISS-E2-2-H	NASA-GISS	USA	v20191120	v20200115	10.22033/ESGF/CMIP6.15861
GISS-E2-1-H	NASA-GISS	USA	v20190403	v20190403	10.22033/ESGF/CMIP6.1421
MIROC6	MIROC	Japan	v20181212	v20190705	10.22033/ESGF/CMIP6.881
NorESM2-LM	NCC	Norway	v20190815	v20210118	10.22033/ESGF/CMIP6.502

2.2 Data processing

Taking ERA5 as an example (a similar analysis is done for the GCMs data), the analysis is based on a two-step approach: (1) Calculation of monthly means. Monthly mean values of cloud radiative effects are derived as follows: CRE_{SW} is calculated as the difference between TSR and TSRC; CRE_{LW} is calculated as the difference between TTR and TTRC; and CRE_{net} is obtained by summing CRE_{SW} and CRE_{LW}. The monthly Global Mean Surface Temperature (GMST) is calculated as the area-weighted mean of air temperature at 2 meters over the globe. The Oceanic Niño Index (ONI) is calculated as the area-weighted, 3-month running mean of sea surface temperature anomalies over the Niño 3.4 region (5° S–5° N, 170° W–120° W). (2) Calculation of monthly deseasonalized anomalies. Anomalies of CRE_{SW}, CRE_{LW}, CRE_{net}, and GMST are calculated as deviations of each variable from its monthly mean, over the entire 72-year period. In the analysis of the GCM simulations data, the ONI is calculated with air temperature at 2 meters.

https://doi.org/10.5194/egusphere-2025-2574
Preprint. Discussion started: 13 June 2025

The spatial averages are calculated taking into consideration the area of the grid cells to account for a decreased contribution of smaller grids. The area of each grid box is estimated as the product of arc length at the corresponding latitude and longitude, considering the Earth as an oblate spheroid with a radius of 6,378.137 km at the equator and 6,356.752 km at the poles. The statistical significance of temporal trends and partial coefficients is assessed using the Hamed and Rao modified Mann-Kendall trend test (Hamed and Rao, 1998; Hussain and Mahmud, 2019) and the Student's t-test, respectively. The Mann-Kendall test is a non-parametric method that accounts for serial autocorrelation.

2.3 The deENSO method

A deENSO procedure is used to remove the ENSO signal from cloud radiative effects and GMST records. Several methods have been developed for this purpose, including those based on numerical simulations and statistical tools such as frequency bandpass filter, regression, and signal decomposition (Penland and Matrosova, 2006; Compo and Sardeshmukh, 2010; Kelly and Jones, 1996; Angell, 2000; Guan and Nigam, 2008). Each method has its strengths and limitations (Compo and Sardeshmukh, 2010).

In this study, we use a regression-based deENSO approach due to its simplicity and efficiency. Specifically, we first use a bandpass filter to remove ONI variations beyond ENSO's typical periodicities (i.e., 2–7 years; Fig. 1) for decoupling signatures of other climate phenomena (e.g., aerosol emission, land use, Pacific Decadal Oscillation and so on) on ONI. Then we use an Ordinary Least Squares (OLS) regression to build statistical relationship between a dependent variable (Y; e.g., CRE_{SW}, CRE_{LW}, CRE_{net} and GMST) and the independent variables of time and the bandpass-filtered ONI, with no time delay. This results in a multivariate regression model (i.e., $\hat{Y} = a \times time + b \times ONI_{filtered} + c$; Eq.1) that minimizes the sum of squared residuals (Virtanen et al., 2020). Therefore, the residual calculated from this model (referred to as deENSO, i.e., $Y_{deENSO} = Y - b \times ONI_{filtered}$; Eq.2) removes the linear ENSO signature while preserving the underlying temporal trend in Y as much as possible. Importantly, this OLS-regression-based deENSO procedure retains both non-linear and delayed components of ENSO-related variations, as well as the ENSO-induced long-term (outside 7 years) trend effect on Y, leading to conservative estimations (Kelly and Jones, 1996; Compo and Sardeshmukh, 2010).

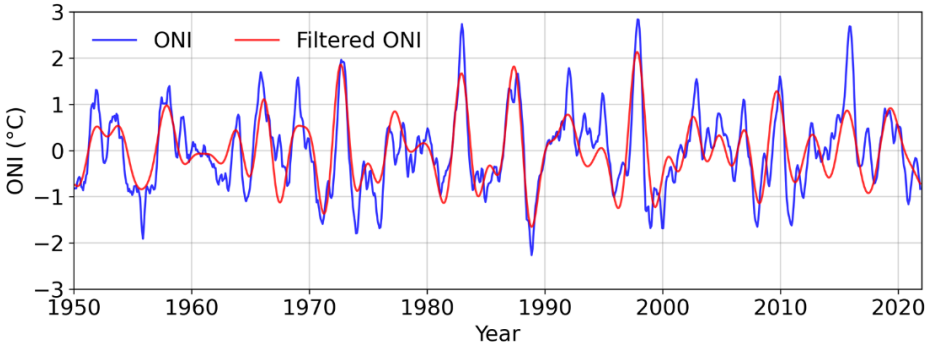

Figure 1: Time series of the original ONI (blue curve) and the bandpass-filtered ONI (red curve) using ERA5 data during the period 01.1950–12.2021.2.4 The estimation of ENSO-related bias

https://doi.org/10.5194/egusphere-2025-2574
Preprint. Discussion started: 13 June 2025

To quantify the cloud feedback to global warming, following previous studies (e.g., Clement et al., 2009; Zhou et al., 2015; Uribe et al., 2022; Ceppi and Nowack et al., 2021; Dessler, 2010), we use a common method that calculates the OLS correlation slope between cloud-related properties and surface temperature (e.g., $\frac{\partial CRE}{\partial GMST}$). Such a method inherently captures the influence of factors affecting both temperature and cloud properties, such as ENSO. To assess the corresponding ENSO-related bias, we compute the difference between the results obtained before and after applying the deENSO procedure. This difference is then used as a proxy measure of the ENSO-related bias in cloud feedback estimates under global warming (i.e., $bias = \frac{\partial CRE}{\partial GMST} - \frac{\partial CRE_{deENSO}}{\partial GMST_{deENSO}}$; Eq.3).

3 Results

3.1 ENSO's impact on the global mean surface temperature

Figure 2 examines the impact of ENSO on GMST using ERA5 data from January 1950 to December 2021.

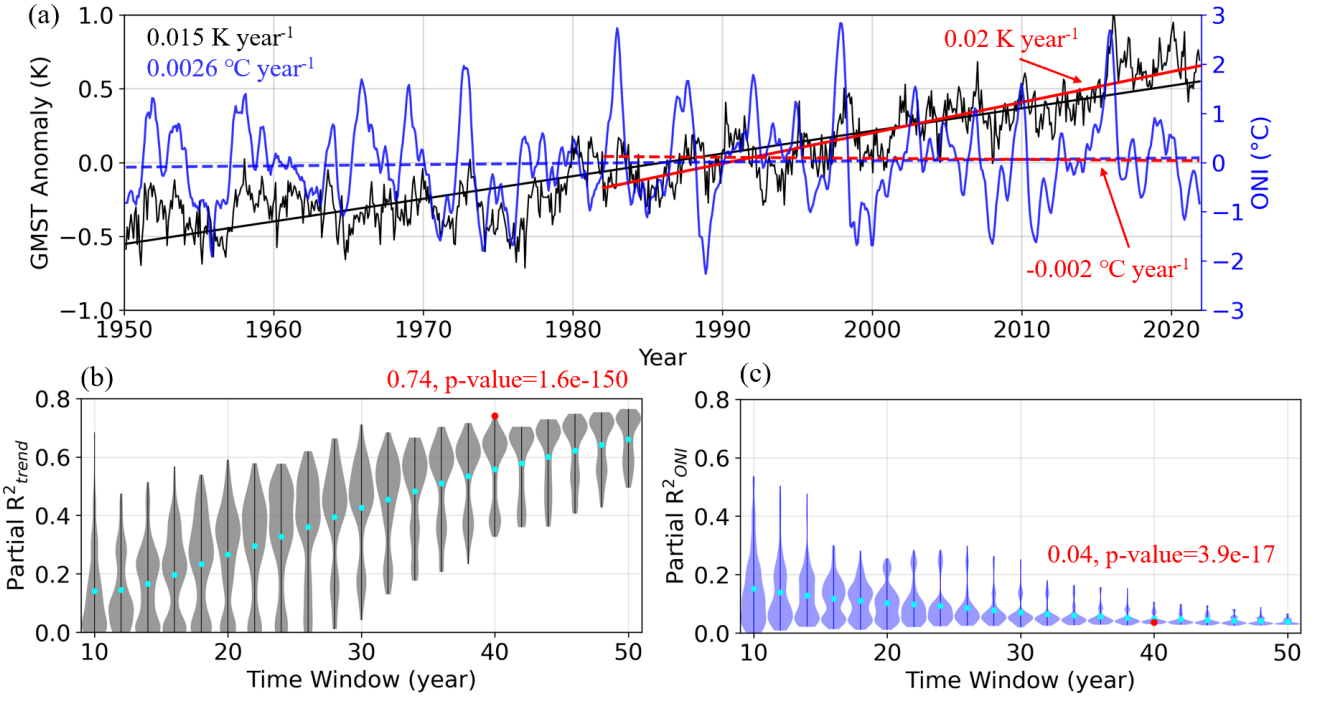

Figure 2: Analysis of the GMST variations driven by the warming trend and ENSO during the period 01.1950–12.2021. (a) Time series of GMST anomaly (black curve; left y-axis) and ONI (blue curve; right y-axis). The black and blue line and number present the corresponding OLS regression line and slope, respectively. (b–c) Violin plots of (b) partial R^2_{trend} and (c) partial R^2_{ONI} for GMST, shown as a function of the time window (in intervals of 2 years). Per time window, the vertical line marks the range (minimal to maximal), the shaded area represents the probability density, and the cyan dot marks the mean value. In this figure, the red lines, dots and numbers highlight the results for the randomly selected 40-year period (1.1982–12.2021) that is analyzed in Fig. 2 and Fig. 4a–f. Solid and dashed lines in panel (a) represent the statistically significant and insignificant trends at a 95% confidence level, respectively.

https://doi.org/10.5194/egusphere-2025-2574
Preprint. Discussion started: 13 June 2025

Figure 2a presents the time series of GMST anomalies (black curve) and the ONI (blue curve). The corresponding OLS regression analysis reveals a consistent increase in GMST of 0.015 K year^{-1} (black line), which translates to an approximate 1 K of warming over the study period. This warming has been primarily attributed to rising CO_2 levels resulting from human activities (Eyring et al., 2021). In contrast, the ONI does not exhibit a significant trend (blue dashed line), indicating no consistent strengthening or weakening of ENSO's intensity in recent decades. This finding aligns with 3 of the 12 GCMs (GISS-E2-2-H, TaiESM1 and E3SM-1-0), which also show no significant ENSO trend in the corresponding historical experiment from 1950 to 2014. However, despite the lack of a long-term trend in ENSO, there is a clear covariation between GMST and ONI on seasonal to interannual timescales, highlighting ENSO's significant impact on GMST. For example, the GMST difference between the La Niña year of 1989 and the El Niño year of 1998 is approximately 0.8 K, a magnitude which is similar to the total warming over the entire 72-year study period.

Of course, the contributions of the warming trend and ENSO to the GMST depend on the analyzed timescale. To quantify this, we calculate the coefficient of partial determination (R^2) using OLS multivariate regression models and present the results as a function of the time window (ranging between 10 to 50 years, with a 2-year interval, the upper limit of 50 years was selected to ensure a sufficient sampling number). This allows us to assess the influence of the warming trend on GMST while controlling ONI (partial R^2_{trend}, Fig. 2b) and the influence of ONI on GMST while controlling the warming trend (partial R^2_{ONI}, Fig. 2c). As shown, the partial R^2_{trend} values increase with longer time windows, suggesting that the warming trend explains a growing portion of GMST variance over extended periods. In contrast, the partial R^2_{ONI} values decrease, indicating that the impact of ENSO diminishes as the timescale lengthens. This inverse relationship implies that ENSO-related bias in cloud feedback estimates decreases for longer periods. Taking a randomly selected 40-year period (01.1982–12.2021; red dots in Fig. 2b–c) as an example, while the warming trend explains approximately 74% of GMST variance, the ENSO-explains only about 4%. Please note that we conducted a similar analysis using six other ENSO indexes to account for the potential limitations of ONI in fully representing ENSO (Johnson, 2013) and got similar results (not shown).

3.2 ENSO's impact on cloud radiative effects

The results presented in Fig. 2 demonstrate the known difference in time scales between the short periodicity of ENSO and the persistent longer warming trend, over recent decades. This known difference led in the past to the neglect of the ENSO-related bias when estimating cloud feedback over long periods. This assumption does not take into account the stronger impact of ENSO on clouds' properties compared to the impact of the warming effect (Li et al., 2021; Liu et al., 2023). To further investigate this point, we analyze the same 40-year period (01.1982–12.2021) and present the partial R^2 maps between cloud radiative effects and the ENSO, and warming signals (Fig. 3) as an example.

https://doi.org/10.5194/egusphere-2025-2574
Preprint. Discussion started: 13 June 2025

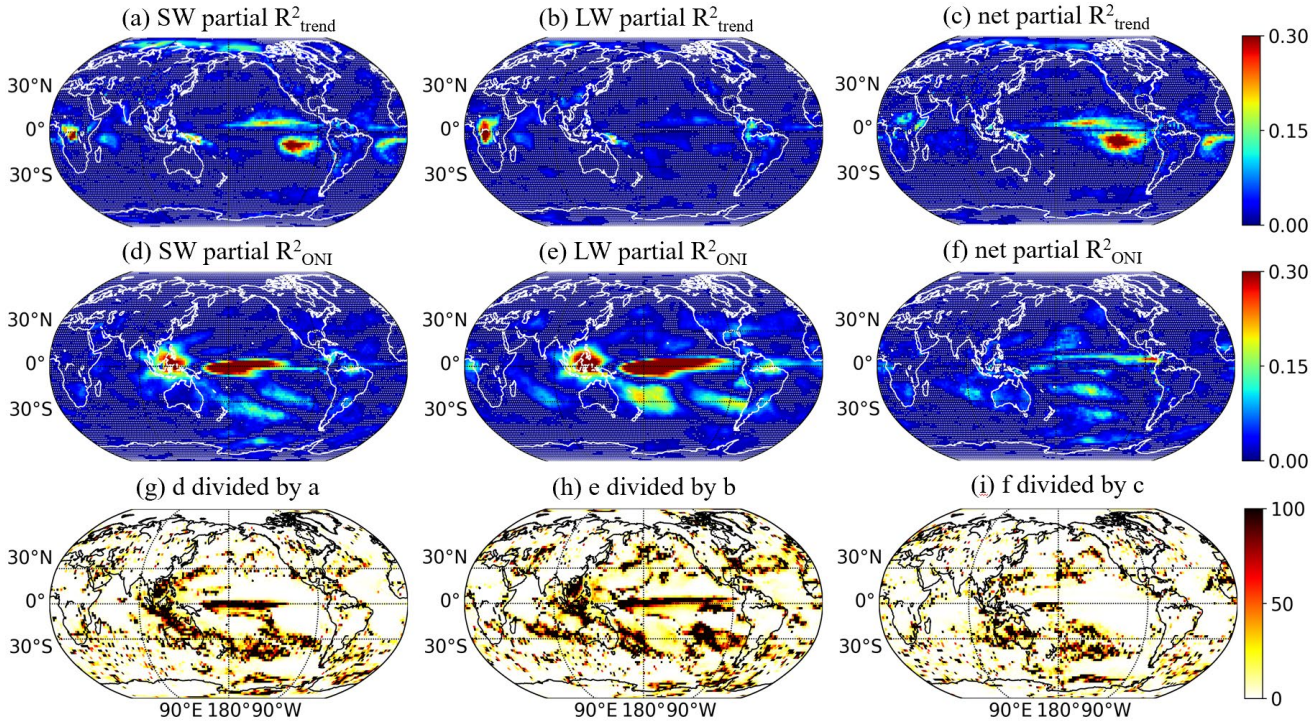

Figure 3: Analysis of the variations in cloud radiative effects as driven by the warming trend and ENSO, taking the period of 01.1982–12.2021 as an example. (a–c) Variations driven by the warming trend (partial R^2_{trend}) in (a) CRE_{SW}, (b) CRE_{LW}, and (c) CRE_{net}. (d–f) Variations driven by ENSO (partial R^2_{ONI}) in (d) CRE_{SW}, (e) CRE_{LW}, and (f) CRE_{net}. (g–i) The ratio between (d–f) and (a–c).

Figure 3a–c presents the spatial distribution of variations in CRE_{SW}, CRE_{LW}, and CRE_{net} attributed to the warming trend while controlling ONI (partial R^2_{trend}). The resulting patterns highlight strong co-variations between clouds and the warming trend in regions such as the Arctic, Middle Africa, and the tropical eastern oceans. Figure 3d–f illustrates the variations in cloud radiative effects driven by ENSO while controlling the warming trend (partial R^2_{ONI}). Figure 3g–i displays the ratio between the two, the partial R^2_{ONI} and R^2_{trend} (Fig. 2d–f divided by Fig. 2a–c). It's clear that, compared to the warming trend, although the ENSO has a much smaller impact on the GMST during this period, the ENSO's impact on cloud radiative effects over a large portion of low- to middle-latitude oceans is significantly stronger. And this is particularly evident across the Pacific, where the ratio reaches values around 100 (blackish shades in Fig. 3g–i), implying a region-dependent ENSO-related bias in the estimation of long-term cloud feedback to global warming.

3.3 ENSO-related bias in estimating historical cloud feedback to global warming

Next, we examine the ENSO-related bias in cloud feedback estimates. Following the deENSO method (Section 2.3), Fig. 4a–f presents the ENSO-related bias calculated for the same exampled 40-year period (01.1982–12.2021).

https://doi.org/10.5194/egusphere-2025-2574
Preprint. Discussion started: 13 June 2025

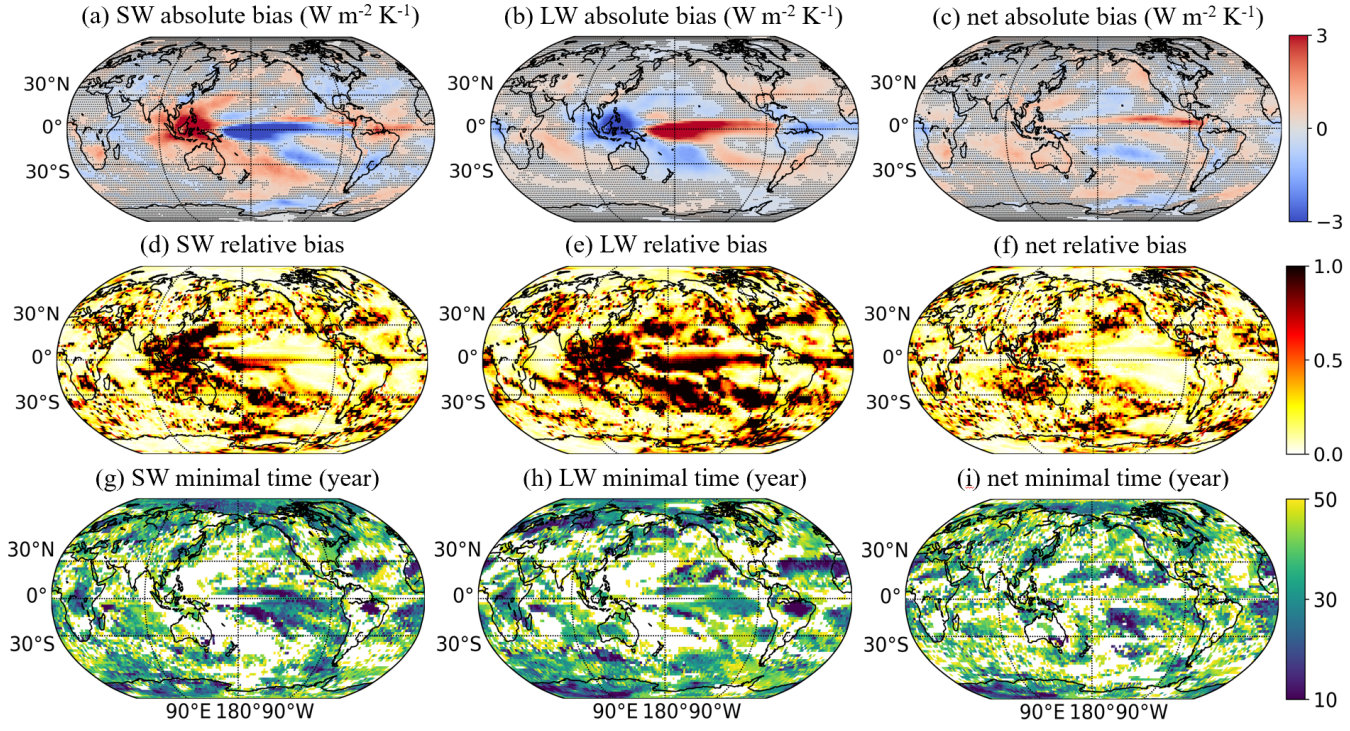

Figure 4: Spatial distributions and timescales of the ENSO-related bias in cloud feedback estimates for different cloud radiative effects, taking the period of 01.1982–12.2021 as an example. (a–c) Maps of the absolute ENSO-related bias in (a) CRE_{SW}, (b) CRE_{LW}, and (c) CRE_{net}. (d–f) Maps of the relative ENSO-related bias (the absolute bias divided by the cloud feedback estimates) in (d) CRE_{SW}, (e) CRE_{LW}, and (f) CRE_{net}. (g–i) Maps of the "ENSO effect minimal time" for (g) CRE_{SW}, (h) CRE_{LW}, and (i) CRE_{net}.

The absolute bias shown in Fig. 4a–c can be explained by the combined effects of ONI-explained variations in GMST (4%) and cloud radiative effects, as discussed in Figs. 2–3. Furthermore, the resulting patterns align closely with previous studies revealing ENSO's influence on cloud properties (Yang et al., 2016; Li et al., 2021; Liu et al., 2023) and the associated physical mechanisms (Taschetto et al., 2020). During the warm phase of ENSO (e.g., El Niño events), the anomalous warming of surface waters in the central to eastern tropical Pacific weakens the Walker circulation, suppressing updrafts over the western Pacific while enhancing convection over the central to eastern Pacific. These dynamic changes affect cloud formation and development, resulting in a larger (smaller) cloud fraction with colder (warmer) cloud top temperatures over regions such as the central (western) tropical Pacific. Consequently, ENSO-driven changes in cloud properties lead to a negative (positive) bias in shortwave cloud feedback estimates over the corresponding regions (Fig. 4a) and an almost opposite one for longwave (Fig. 4b), together leading to relatively weak and less distinct bias in the net cloud feedback estimates (Fig. 4c). Such consistency further validates the reliability of our regression-based deENSO method. Figure 4 d–f shows the distributions of the relative ENSO-related bias. As expected, the ratio reaches 1 (blackish shades) over a substantial part of low- to mid-latitude oceans, indicating comparable ENSO- and non-ENSO-forced cloud feedback over these regions.

https://doi.org/10.5194/egusphere-2025-2574
Preprint. Discussion started: 13 June 2025

As mentioned in Fig. 2, the impact of ENSO on GMST varies depending on the period under examination. To quantify it, we calculate the relative ENSO-related bias (e.g., Fig. 4d–f) for the same range of possible periods by applying each time window across the entire 72 years and introduce the concept of "ENSO effect minimal time". This metric is defined as the shortest time window (and all longer time windows), for which, the mean magnitude of the relative bias (ignoring the sign) is smaller than 0.5 (i.e., $\left|\overline{relative\ bias}\right| < 0.5$). This definition indicates that for periods longer than the "ENSO effect minimal time", the ENSO-related bias in cloud feedback is expected to be smaller than the non-ENSO part. Figure 4g–i presents the "ENSO effect minimal time" maps for CRE_{SW}, CRE_{LW}, and CRE_{net}, revealing complex patterns and notable differences among the three variables. In most regions, the minimal time is shorter than the maximal time window in this study (50 years). However, in some tropical regions, particularly over the Pacific, the mean relative bias is never consistently below 0.5 within time windows up to 50 years (marked by white shades).

These results illustrate clearly that ENSO drives a significant bias in the assessment of long-term cloud feedback to global warming, especially over the Pacific or during relatively short periods characterized by intense ENSO activity. To partly validate our findings, taking the CRE_{net} as an example, we analyzed the "ENSO effect minimal time" for 12 GCM simulations of the historical experiments (Fig 5). Though obvious discrepancies exist, the general message of these results is that the ENSO can significantly bias long-term cloud feedback estimates. The discrepancies between the models indicate deficiencies in the ability of models to accurately represent the ENSO, global warming, and their relative impacts on GMST and clouds properties (Bellenger et al., 2014; Coburn and Pryor, 2021).

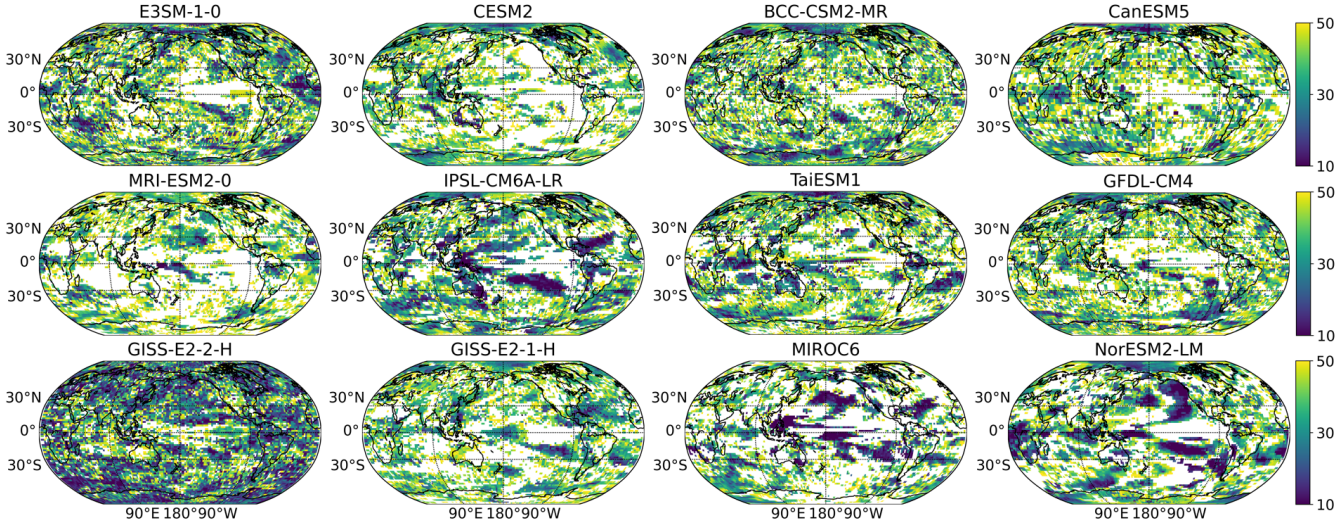

Figure 5: Maps of the "ENSO effect minimal time" for CRE_{net} from the CMIP6 historical experiment during 01.1950–12.2014. The name of the corresponding model is titled.

https://doi.org/10.5194/egusphere-2025-2574
Preprint. Discussion started: 13 June 2025

3.4 ENSO-related bias in estimating cloud feedback with the abrupt-4×CO_2 experiment

To link our findings to climate projections, we analyze the abrupt-4×CO_2 GCM experiment data, using the first 150 years of simulations. Figures 6 and 7 give the absolute and relative bias in CRE_{net}, respectively.

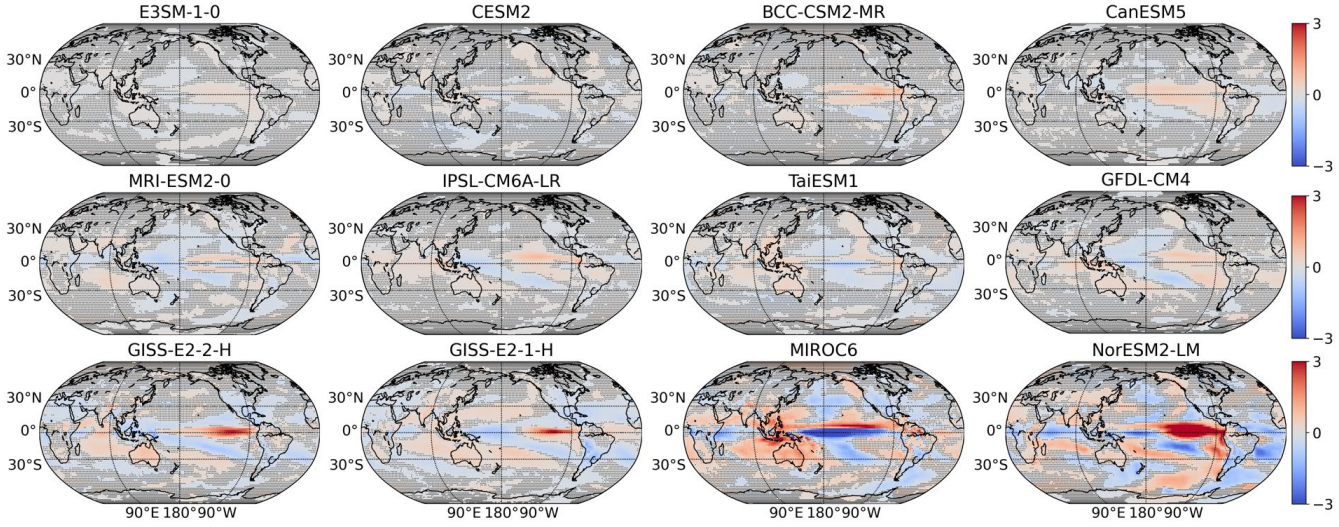

Figure 6: Maps of the absolute ENSO-related bias in CRE_{net} from the abrupt-4×CO_2 experiment during the first 150 years. The name of the corresponding model is titled.

Again, on one hand, significant ENSO-related biases are captured worldwide, especially over the Pacific Ocean; on the other hand, obvious discrepancies in terms of both patterns and magnitudes exist among GCMs. More specifically, Fig. 6 suggests an overall positive bias (reddish shades) over the eastern tropical Pacific and an overall negative bias (bluish shades) over the western tropical Pacific, indicating that GCMs captured the typical pattern of cloud response to ENSO to a certain degree. But the corresponding magnitudes vary dramatically between the 12 models, GCMs like MIROC6 and NorESM2-LM even show that the absolute ENSO-related bias in cloud feedback estimates over 150 years reaches a few W m^{-2} K^{-1} over a large portion of the world, which is comparable to the local cloud feedback estimations (Forster et al., 2021; Ceppi & Nowack, 2021; Zelinka et al., 2016; Myers et al., 2021).

https://doi.org/10.5194/egusphere-2025-2574
Preprint. Discussion started: 13 June 2025

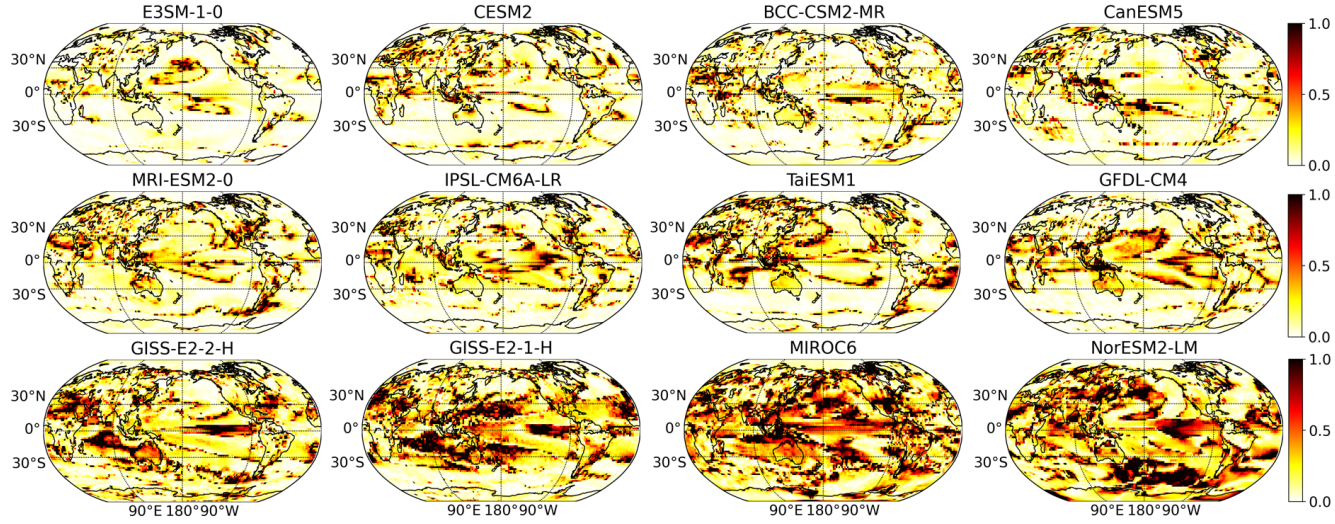

Figure 7: Maps of the relative ENSO-related bias in CRE_{net} from the abrupt-4×CO_2 experiment during the first 150 years. The name of the corresponding model is titled.

Compared to the absolute bias, the relative bias (Fig. 7) shows even more significant model uncertainties regarding both the pattern and the magnitude. As discussed before, these differences indicate deficiencies of models in accurately representing the ENSO, global warming, and their relative impacts on GMST and clouds (Bellenger et al., 2014; Coburn and Pryor, 2021). For example, previous studies suggest that, compared to observations, current GCMs present a too-strong equatorial Pacific cold tongue (Jiang et al., 2021) and fail to capture the recent strengthening of the west-to-east equatorial Pacific SST gradient (Seager et al., 2019). These two deficiencies introduce critical uncertainties in the projection of ENSO, and hence clouds, under global warming (e.g., Guilyardi et al., 2020; Beobide-Arsuaga et al., 2021).

4 Discussion

ENSO is a natural interannual climate phenomenon associated with anomalous sea surface temperature and pressure in the tropical Pacific Ocean. It has been shown to impact global temperature and cloud properties (Davey et al., 2014; Cai et al., 2019; Taschetto et al., 2020), and consequently, it affects the accuracy of cloud feedback estimates under global warming (Zhou et al., 2015; Uribe et al., 2022; Richardson et al., 2022; Jin et al., 2024). This study uses 72 years of ERA5 data and long-term simulations by 12 GCMs to quantify such ENSO-related biases. The results reveal that regression-based cloud feedback estimations are susceptible to a significant ENSO-related bias, even over decades. A regression-based deENSO procedure was then applied to quantify the bias. The findings show that the magnitude of the bias varies across different regions and timescales. In most regions, ENSO-related bias is smaller than the non-ENSO part only over timescale of decades. However, in many tropical regions, the bias can exceed the non-ENSO part, even for periods longer than 50 years (the maximal time window analyzed). These results highlight the importance of incorporating a deENSO procedure when estimating climate trends, particularly over the Pacific Ocean or during periods of intense ENSO activity.

https://doi.org/10.5194/egusphere-2025-2574
Preprint. Discussion started: 13 June 2025

The study acknowledges several limitations, including its inability to account for non-linear or delayed ENSO effects (Compo and Sardeshmukh, 2010) and the sensitivity of the 'ENSO effect minimal time' to models. As a result, the findings should be considered conservative estimates and the quantitative conclusions should be interpreted with caution, particularly in the context of GCM simulations. Despite these limitations, the study provides a straightforward method to approximate ENSO-related biases, offering valuable insights into the influence of ENSO on cloud feedback estimates. The implications of this research are significant. First, it quantifies the distribution and timescales of the ENSO-related bias in cloud feedback estimates. Second, given the known deficiencies in GCMs' representation of ENSO and its dynamics (Bellenger et al., 2014; Coburn and Pryor, 2021; Jiang et al., 2021; Seager et al., 2019), as well as uncertainties in future ENSO projections (Guilyardi et al., 2020; Beobide-Arsuaga et al., 2021), the revealed significant impact of ENSO on warming and cloud properties highlight critical challenges to the reliability of climate projections.

References

Angell, J. K.: Tropospheric temperature variations adjusted for El Niño, 1958–1998, J. Geophys. Res. Atmos., 105, 11841–11849, doi:10.1029/2000JD900044, 2000.

Bellenger, H., Guilyardi, E., Leloup, J., Lengaigne, M. and Vialard, J.: ENSO representation in climate models: From CMIP3 to CMIP5, Clim. Dyn., 42, 1999–2018, doi:10.1007/s00382-013-1783-z, 2014.

Beobide-Arsuaga, G., Bayr, T., Reintges, A. and Latif, M.: Uncertainty of ENSO-amplitude projections in CMIP5 and CMIP6 models, Clim. Dyn., 56, 3875–3888, doi:10.1007/s00382-021-05673-4, 2021.

Binder, H., Boettcher, M., Joos, H., Sprenger, M. and Wernli, H.: Vertical cloud structure of warm conveyor belts–a comparison and evaluation of ERA5 reanalysis, CloudSat and CALIPSO data, Weather Clim. Dyn., 1, 577–595, doi:10.5194/wcd-1-577-2020, 2020.

Cai, W. et al.: Pantropical climate interactions, Science, 363, eaav4236, doi:10.1126/science.aav423, 2019.

Ceppi, P. and Nowack, P.: Observational evidence that cloud feedback amplifies global warming, Proc. Natl. Acad. Sci., 118, e2026290118, doi:10.1073/pnas.2026290118, 2021.

Chen, T., Rossow, W.B., and Zhang, Y.: Radiative effects of cloud-type variations, J. Clim., 13, 264–286, doi:10.1175/1520-0442(2000)013<0264:REOCTV>2.0.CO;2, 2000.

Clement, A. C., Burgman, R. and Norris, J. R.: Observational and Model Evidence for Positive Low-Level Cloud Feedback, Science, 325, 460–464, doi:10.1126/science.11712, 2009.

Coburn, J. and Pryor, S. C.: Differential Credibility of Climate Modes in CMIP6, J. Clim., 34, 8145–8164, doi:10.1175/JCLI-D-21-0359.1, 2021.

Compo, G. P. and Sardeshmukh, P. D.: Removing ENSO-related variations from the climate record, J. Clim., 23, 1957–1978, doi:10.1175/2009JCLI2735.1, 2010.

https://doi.org/10.5194/egusphere-2025-2574
Preprint. Discussion started: 13 June 2025

Davey, M., Brookshaw, A. and Ineson, S.: The probability of the impact of ENSO on precipitation and near-surface temperature, Clim. Risk Manag., 1, 5–24, doi:10.1016/j.crm.2013.12.002, 2014.

Dessler, A. E.: A determination of the cloud feedback from climate variations over the past decade, Science, 330, 1523–1527, doi:10.1126/science.1192546, 2010.

Eleftheratos, K., Zerefos, C., Varotsos, C. and Kapsomenakis, I.: Interannual variability of cirrus clouds in the tropics in el niño southern oscillation (ENSO) regions based on international satellite cloud climatology project (ISCCP) satellite data, Int. J. Remote Sens., 32, 6395–6405, doi:10.1080/01431161.2010.510491, 2011.

Eyring, V., Bony, S., Meehl, G. A., Senior, C. A., Stevens, B., Stouffer, R. J., and Taylor, K. E.: Overview of the Coupled Model Intercomparison Project Phase 6 (CMIP6) experimental design and organization, Geosci. Model Dev., 9, 1937–1958, doi:10.5194/gmd-9-1937-2016, 2016.

Eyring, V., Gillett, N. P., Achuta Rao, K. M., Barimalala, R., Barreiro Parrillo, M., Bellouin, N. et al.: Human Influence on the Climate System, in Climate Change 2021: The Physical Science Basis, Contribution of Working Group I to the Sixth Assessment Report of the Intergovernmental Panel on Climate Change (Cambridge University), doi:10.1017/9781009157896.005, 2021.

Forster, P., Storelvmo, T., Armour, K., Collins, W., Dufresne, J. L., Frame, D. et al.: The Earth's Energy Budget, Climate Feedbacks, and Climate Sensitivity, in Climate Change 2021: The Physical Science Basis, Contribution of Working Group I to the Sixth Assessment Report of the Intergovernmental Panel on Climate Change (Cambridge University), doi:10.1017/9781009157896.009, 2021.

Glantz, M. H. and Ramirez, I. J.: Reviewing the oceanic Nino index (ONI) to enhance societal readiness for El Niño's impacts, Int. J. Disaster Risk Sci., 11, 394–403, doi:10.1007/s13753-020-00275-w, 2020.

Guan, B. and Nigam, S.: Pacific Sea Surface Temperatures in the Twentieth Century: An Evolution-Centric Analysis of Variability and Trend, J. Clim., 21, 2790–2809, doi:10.1175/2007JCLI2076.1, 2008.

Guilyardi, E., Capotondi, A., Lengaigne, M., Thual, S. and Wittenberg, A. T.: ENSO Modeling: History, Progress, and Challenges, in El Niño Southern Oscillation in a Changing Climate (American Geophysical Union), doi:10.1002/9781119548164.ch9, 2020.

Gulev, S. K., Thorne, P. W., Ahn, J., Dentener, F. J., Domingues, C. M., Gong, D. et al.: Changing State of the Climate System, in Climate Change 2021: The Physical Science Basis, Contribution of Working Group I to the Sixth Assessment Report of the Intergovernmental Panel on Climate Change (Cambridge University), doi:10.1017/9781009157896.004, 2021.

Hamed, K. H. and Rao, A. R.: A modified Mann-Kendall trend test for autocorrelated data, J. Hydrol., 204, 182-196, doi:10.1016/S0022-1694(97)00125-X, 1998.

Hersbach, H., Bell, B., Berrisford, P., Hirahara, S., Horányi, A., Muñoz-Sabater, J. et al.: The ERA5 global reanalysis, Q. J. R. Meteorol. Soc., 146, 1999–2049, doi:10.1002/qj.3803, 2020.

https://doi.org/10.5194/egusphere-2025-2574
Preprint. Discussion started: 13 June 2025

Hersbach, H. Bell, B., Berrisford, P., Biavati, G., Horányi, A., Muñoz-Sabater, J. et al.: ERA5 monthly averaged data on single levels from 1940 to present [Dataset], Copernicus Climate Change Service (C3S) Climate Data Store (CDS), doi:10.24381/cds.f17050d7, 2023.

Hope, P., Henley, B. J., Gergis, J., Brown, J. and Ye, H.: Time-varying spectral characteristics of ENSO over the Last Millennium, Clim. Dyn., 49, 1705–1727, doi:10.1007/s00382-016-3393-z, 2017.

Hussain, M. M. and Mahmud, I.: pyMannKendall: a python package for non parametric Mann Kendall family of trend tests [Software], J. Open Source Softw., 4, 1556, doi:10.21105/joss.01556, 2019.

Jiang, W., Huang, P., Huang, G. and Ying, J.: Origins of the Excessive Westward Extension of ENSO SST Simulated in CMIP5 and CMIP6 Models, J. Clim., 34, 2839–2851, doi:10.1175/JCLI-D-20-0551.1, 2021.

Jin, D., Kramer R. J., Oreopoulos, L. and Lee D.: ENSO disrupts boreal winter CRE feedback, J. Clim., 37, 585–603, doi:10.1175/JCLI-D-23-0282.1, 2024.

Johnson, N. C.: How many ENSO flavors can we distinguish?, J. Clim., 26, 4816–4827, doi:10.1175/JCLI-D-12-00649.1, 2013.

Kelly, P. M. and Jones, P. D.: Removal of the El Niño-Southern Oscillation signal from the gridded surface air temperature data set, J. Geophys. Res. Atmos., 101, 19013–19022, doi:10.1029/96JD01173, 1996.

Li, Y. et al.: Pairwise-rotated EOFs of global cloud cover and their linkages to sea surface temperature, Int. J. Climatol., 41, 2342–2359, doi:10.1002/joc.6962, 2021.

Liu, H., Koren, I., Altaratz, O. and Chekroun, M. D.: Opposing trends of cloud coverage over land and ocean under global warming, Atmos. Chem. Phys., 23, 6559–6569, doi:10.5194/acp-23-6559-2023, 2023.

Madenach, N., Carbajal Henken, C., Preusker, R., Sourdeval, O. and Fischer, J.: Analysis and quantification of ENSO-linked changes in the tropical atlantic cloud vertical distribution using 14 years of MODIS observations, Atmos. Chem. Phys., 19, 13535–13546, doi:10.5194/acp-19-13535-2019, 2019.

Myers, T. A., Scott, R. C., Zelinka, M. D., Klein, S. A., Norris, J. R. and Caldwell, P. M.: Observational constraints on low cloud feedback reduce uncertainty of climate sensitivity, Nat. Clim. Chang., 11, 501–507, doi:10.1038/s41558-021-01039-0, 2021.

Neelin, J. D., Battisti, D. S., Hirst, A. C., Jin, F. F., Wakata, Y., Yamagata, T. et al.: ENSO theory, J. Geophys. Res.: Oceans, 103, 14261–14290, doi:10.1029/97JC03424, 1998.

Park, S. and Leovy C. B.: Marine low-cloud anomalies associated with ENSO, J. Clim., 17, 3448–3469, doi:10.1175/1520-0442(2004)017<3448:MLAAWE>2.0.CO;2, 2004.

Penland, C. and Matrosova, L.: Studies of El Niño and interdecadal variability in tropical sea surface temperatures using a nonnormal filter, J. Clim., 19, 5796–5815, doi:10.1175/JCLI3951.1, 2006.

Richardson, M. T., Roy, R. J. and Lebsock, M. D.: Satellites suggest rising tropical high cloud altitude: 2002–2021, Geophys. Res. Lett., 49, e2022GL098160, doi:10.1029/2022GL098160, 2022.

https://doi.org/10.5194/egusphere-2025-2574
Preprint. Discussion started: 13 June 2025

Seager, R., Cane, M., Henderson, N., Lee, D. E., Abernathey, R. and Zhang, H.: Strengthening tropical Pacific zonal sea surface temperature gradient consistent with rising greenhouse gases, Nat. Clim. Chang., 9, 517-522, doi:10.1038/s41558-019-0505-x, 2019.

Stephens, G. L., Li, J., Wild, M., Clayson C. A., Loeb, N., Kato, S. et al.: An update on Earth's energy balance in light of the latest global observations, Nat. Geosci., 5, 691–696, doi:10.1038/ngeo1580, 2012.

Stubenrauch, C. J., Rossow, W. B., Kinne S., Ackerman, S., Cesana G., Chepfer, H. et al.: Assessment of global cloud datasets from satellites: Project and database initiated by the GEWEX radiation panel, Bull. Amer. Meteor. Soc., 94, 1031–1049, doi:10.1175/BAMS-D-12-00117.1, 2013.

Taschetto, A. S., Ummenhofer, C. C., Stuecker, M. F., Dommenget, D., Ashok, K., Rodrigues, R. R. et al.: ENSO Atmospheric Teleconnections, in El Niño Southern Oscillation in a Changing Climate (American Geophysical Union), doi:10.1002/9781119548164.ch14, 2020.

Teng, H. F., Lee, C. S. and Hsu, H. H.: Influence of ENSO on formation of tropical cloud clusters and their development into tropical cyclones in the western north pacific, Geophys. Res. Lett., 41, 9120–9126, doi:10.1002/2014GL061823, 2014.

Uribe, A., Bender, F. A. M. and Mauritsen, T.: Observed and CMIP6 modeled internal variability feedbacks and their relation to forced climate feedbacks, Geophys. Res. Lett., 49, e2022GL100075, doi:10.1029/2022GL100075, 2022.

Virtanen, P., Gommers, R., Oliphant, T. E., Haberland M., Reddy, T., Cournapeau, D. et al.: SciPy 1.0: Fundamental Algorithms for Scientific Computing in Python, Nat. Methods, 17, 261-272, doi:10.1038/s41592-019-0686-2., 2020.

Webb, M. J., Andrews, T., Bodas-Salcedo, A., Bony, S., Bretherton, C. S., Chadwick, R. et al.: The Cloud Feedback Model Intercomparison Project (CFMIP) contribution to CMIP6, Geosci. Model Dev., 10, 359-384, doi:10.5194/gmd-10-359-2017, 2017.

Yang, Y., Russell, L. M., Xu, L., Lou, S., Lamjiri, M. A., Somerville, R. C. J. et al.: Impacts of ENSO events on cloud radiative effects in preindustrial conditions: changes in cloud fraction and their dependence on interactive aerosol emissions and concentrations, J. Geophys. Res. Atmos., 121, 6321–6335, doi:10.1002/2015JD024503, 2016.

Yao, B., Teng, S., Lai, R., Xu, X., Yin, Y., Shi, C. et al.: Can atmospheric reanalyses (CRA and ERA5) represent cloud spatiotemporal characteristics?. Atmos. Res., 244, 105091, doi:10.1016/j.atmosres.2020.105091, 2020.

Zelinka, M. D., Zhou, C. and Klein, S. A.: Insights from a refined decomposition of cloud feedbacks, Geophys. Res. Lett., 43, 9259–9269, doi:10.1002/2016GL069917, 2016.

Zelinka, M. D., Myers, T. A., McCoy, D. T., Po-Chedley, S., Caldwell, P. M., Ceppi, P. et al.: Causes of higher climate sensitivity in cmip6 models, Geophys. Res. Lett., 47, 2019–085782, doi:10.1029/2019GL085782, 2020.

Zhou, C., Zelinka, M. K., Dessler, A. E., and Klein S. A.: The relationship between interannual and long-term cloud feedbacks, Geophys. Res. Lett., 42, 10–463, doi:10.1002/2015GL066698, 2015.